Thermal Stability of Flame-Synthesized Anatase TiO_2 Nanoparticles

John R. McCormick,[†] Bin Zhao,[‡,||] Sergey A. Rykov,[§] Hai Wang,[‡,||] and Jingguang G. Chen*[,§]

Departments of Materials Science and Engineering, Mechanical Engineering, and Chemical Engineering, University of Delaware, Newark, Delaware 19716

Received: July 14, 2004; In Final Form: September 1, 2004

The thermal stability of anatase TiO_2 nanoparticles, produced by flame synthesis, is investigated in the current study. Phase-pure anatase particles of ~4 nm in size can be reproducibly synthesized by using a tubular burner and rotating sampler. Transmission electron microscopy (TEM), glancing incidence X-ray diffraction (XRD), and near-edge X-ray absorption fine structure (NEXAFS) were utilized to characterize the particles before and after annealing to various temperatures. TEM investigations reveal a primary particle size of ~4 nm with standard deviations around 1 nm. XRD and selected area electron diffraction (SAED) indicate that TiO_2 nanoparticles are phase-pure anatase. Our results indicate that the particles remain kinetically trapped upon annealing up to 773 K in air for 2 h. At 973 K, increases in average size, rutile content, and particle shape are observed, consistent with recent reports in the literature. NEXAFS measurements indicate that the O K-edge features of the nanoparticles show similarities to those of surfaces of bulk TiO_2.

I. Introduction

TiO_2 has long been known to be an active heterogeneous catalyst and photocatalyst. In addition, it is used in solar cells, gas sensors, pigments, and various devices.[1] The nanoparticle TiO_2 is used in the photocatalytic removal of pollutants from wastewater and air.[2] Due to a large specific surface area and high active-site density, nanometer sized particles are becoming increasingly attractive catalysts. In addition, TiO_2 shows a quantum size effect that can influence both the mechanical and chemical properties.[3] For example, for TiO_2 particles with sizes smaller than ~20 nm, there is a sharp increase in the catalytic activity.[4−6]

The utilization of combustion flame synthesis has shown the promise of synthesizing nanoparticles in the desired size range with a uniform size distribution.[7,8] Extensive studies have been conducted on flame-synthesized particles larger than 10 nm.[9−11] Optimization of the process parameters can yield particles as small as 3 nm within a narrow size distribution, performing better than many other techniques for particle synthesis.[7,8,10,12,13] Woolridge[13] and Pratsinis[10] have provided excellent reviews of this topic. Studies have shown that the particle size is influenced by a variety of parameters prior to the flame as well as in the flame; however, the process temperature has the most drastic effect on product characteristics such as particle size, morphology, and phase composition.[10] In our studies, precursor concentration or, more specifically, precursor carrier gas flow rate was set as the process control variable, owing to ease of control.

TiO_2 particles produced by flame synthesis typically consist of fine, nonporous particles. In addition to size, the synthesis conditions also influence the phase and morphology of the nanoparticles.[10] For example, Kammler et al. showed that the rutile content could be kept as low as 0.1% in a diffusion flame.[14] Skandan et al. showed that the conversion of anatase TiO_2 to rutile occurred at temperatures above 1073 K.[7]

The understanding of the thermal stability of nanoparticles is of critical importance for fundamental surface science and catalytic studies. In surface science studies the sample surfaces are often annealed to elevated temperature for sample preparation or for thermal desorption studies. Catalytic investigations are often carried out at high temperatures. The determination of the thermal studies of TiO_2 would therefore identify a temperature window, within which reproducible surface science and catalytic studies can be performed. The primary objective of the current study is to determine the temperature range to maintain the structural stability of anatase TiO_2 nanoparticles.

II. Experimental Section

Particle synthesis was performed in a custom-built laminar-flow burner operating at atmospheric pressure described previously.[12] Argon carrier gas is bubbled through preheated (373 K) liquid titanium tetraisopropoxide (TTIP) from Sigma-Aldrich with a purity of 97%. The flow rate of the argon carrier gas controls the TTIP concentration in the burner. The precursor gas mixture is then mixed with a fuel mixture containing argon and oxygen (BOC Gases, 99.999%) and ethylene (Matheson, 99.9%). This mixture then enters the burner in a laminar flow regime. Combustion occurs outside the burner where a water-cooled copper flame stop stabilizes the flame. A tungsten−tantalum sample holder attached to a computer-controlled motor, spinning at a constant rotational speed, sweeps through the flame such that the sample is only in the flame for 17 ms in each insertion. TiO_2 particles are deposited on an Al_2O_3 substrate primarily by a thermophoretic effect. The short residence time inside the flame keeps the substrate temperature below 373 K. Flame temperature is measured by using a 125 μm Pt−Pt−10%Rh thermocouple (Type S) coated with a YCl_3/BeO mixture. The maximum flame temperature is 1923 K. The sample holder also contains two slots for insertion of transmission electron microscope (TEM) grids for direct deposition analysis. Online particle size sampling is performed on a TSI Model 3936

* Address correspondence to this author. E-mail: jgchen@udel.edu.
[†] Department of Materials Science and Engineering.
[‡] Department of Mechanical Engineering.
[§] Department of Chemical Engineering.
[||] Present address: Department of Aerospace and Mechanical Engineering, University of Southern California, Los Angeles, California 90089.

10.1021/jp046874f CCC: $27.50
Published on Web 10/20/2004

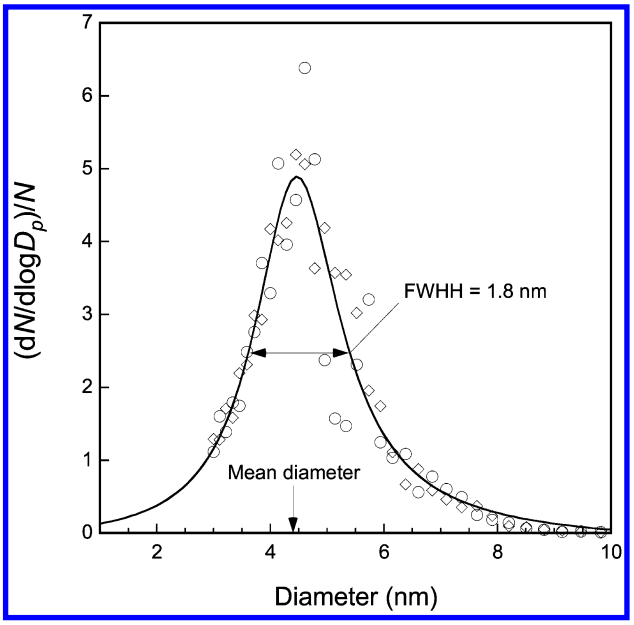

Figure 1. Particle size distribution function measured by SMPS. Symbols represent experimental data and the line is fit to the data.

Scanning Mobility Particle Sizer (SMPS) discussed in detail previously.[16,17] The SMPS can measure particles larger than 3 nm.

TEM characterization was conducted on a JEM 2010F field emission transmission electron microscope operating at an accelerating voltage of 200 kV. The TEM is equipped with an X-ray energy dispersive spectrometer (XEDS), Gatan image filter (GIF), and multiscan CCD camera. Selected area electron diffraction patterns were obtained in conventional diffraction mode with a camera length between 80 and 150 cm.

Glancing incidence XRD was performed on a Rigaku DMAX 2200 diffractometer with an Ultima $\theta-2\theta$ goniometer, in asymmetric parallel-beam condition, with copper Kα X-rays at 40 kV and 40 mA. The diffracted beam is monochromatized with a graphite crystal and the incident beam is held at a fixed angle of 1°.

NEXAFS measurements were performed at the U1A Beamline at the National Synchrotron Light Source (NSLS) at Brookhaven National Labs. Details about the setup can be found in previous publications.[19,20] Electron yield intensities were measured with a channeltron multiplier with a front-end bias of −100 V to reduce signals from secondary electrons. The NEXAFS spectra were measured as a function of the incident X-ray photon energy for the oxygen K-edge region (520−580 eV), with an energy resolution of approximately 0.8 eV.

III. Results

Figure 1 displays SMPS measurements of the particle size distribution function. The particles subject to the current thermal

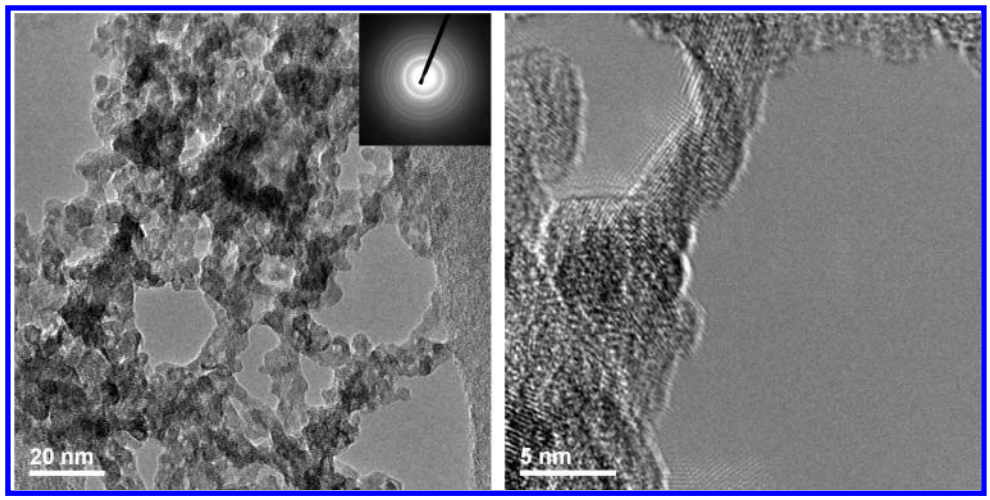

Figure 2. TEM image of TiO_2 nanoparticles prior to annealing: (a) wide-area image of nanoparticles with inserted SAED pattern and (b) high-resolution image of TiO_2 nanoparticles.

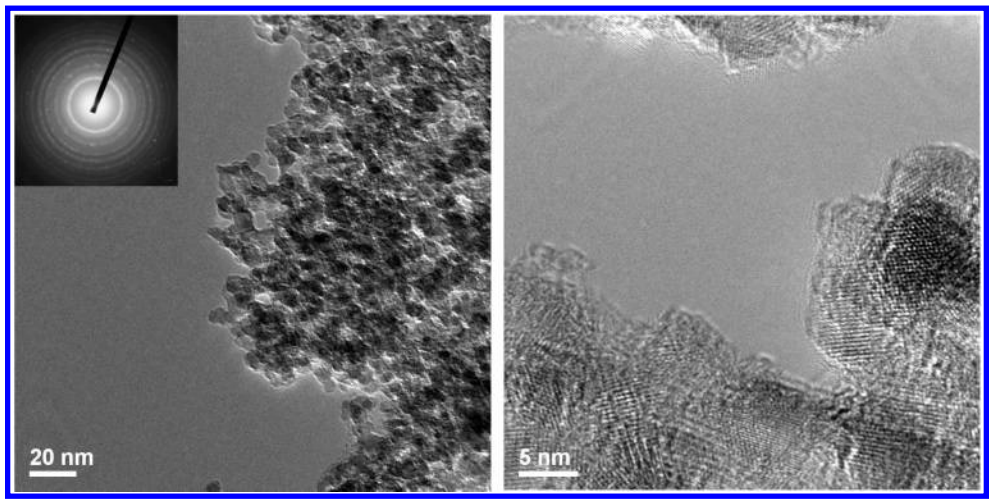

Figure 3. TEM image of TiO_2 nanoparticles after annealing at 773 K for 2 h: (a) wide-area image of nanoparticles with inserted SAED pattern and (b) high-resolution image of TiO_2 nanoparticles.

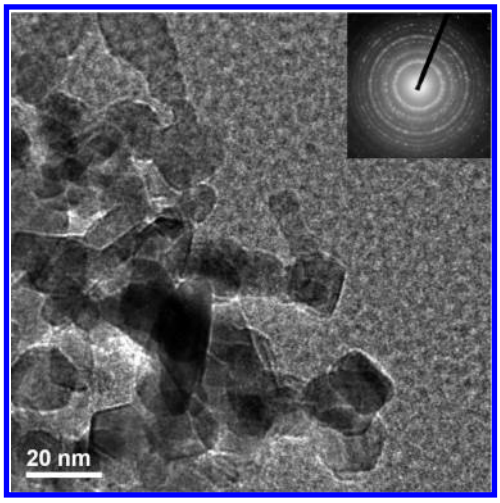

Figure 4. TEM image of TiO_2 nanoparticles after annealing at 973 K for 2h.

TABLE 1

anneal temp (K)	particle size (nm)	std dev (nm)
fresh	4.4	0.9
573	3.7	0.9
673	4.6	1.3
773	4.1	1.0
973	14.3	5.3

studies have a mean diameter of 4 nm. The size variation of the particle sample is quite narrow, as indicated by the full width at half height (fwhh) of 1.8 nm.

The thermal stability of flame-synthesized particles in the size range of ~4 nm was investigated by using TEM, XRD, and NEXAFS. Particles deposited onto an Al_2O_3 substrate were annealed in air for 2 h Annealing temperatures of 573, 673, 773, and 973 K are investigated. Results show that little particle sintering occurs after annealing these samples up to 773 K. Figures 2 through 4 show typical wide-area TEM and high-resolution micrographs for the fresh and 773 and 973 K annealed samples. TEM measurements performed on fresh samples show aggregated particles that are generally spherical in nature. No increase in average size or change in particle shape was seen after annealing up to 773 K. The average particle sizes, estimated from TEM, are listed in Table 1. However, after annealing at 973 K, the sample size drastically increases from approximately 4 to 14 nm average size with a corresponding increase in the standard deviation from 1.0 to 5.3 nm. In addition, a definite change in particle shape occurred leading to more rectangular particles. This shape change is partially responsible for the large increase in the standard deviation, as a spherical assumption is still used in determining the particle size.

SAED patterns, shown as inserts in Figures 2 through 4, are analyzed as follows: Due to the ring nature of the polycrystalline samples, radial intensity profiles are generated by integrating pixel intensities in the angular direction, θ, for constant radius. In this way, intensity vs radius plots can be constructed. After background subtraction, the intensity profile is then converted to real space, and the intensity is displayed vs d spacing. Figure 5 displays the SAED intensity profiles for the inserts in Figures 2 through 4 as well as the theoretical peaks for anatase, brookite, and rutile phases. Annealing to 773 K leads to a slight increase in the anatase (101) centered at 3.52 Å, with a possible shoulder associated with brookite (211) located at 2.90 Å. No rutile formation is observed based on the absence of the rutile (110) and (111) diffraction peaks.

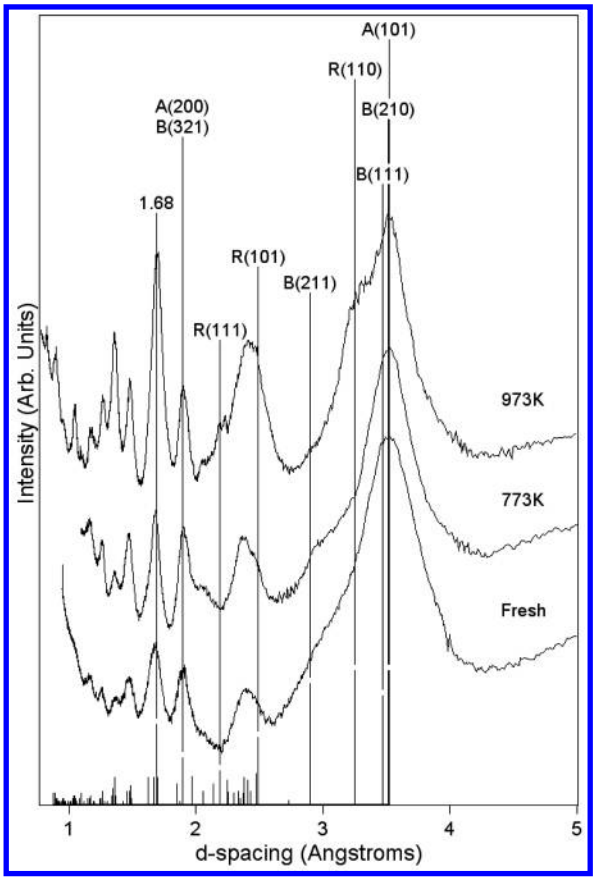

Figure 5. Real-space transform of SAED patterns of TiO_2 particles before and after annealing as shown in Figures 2−4. Calculated rutile, brookite, and anatase peaks are included.

After annealing to 973 K there is a sharp increase in the shoulder of the anatase (101) due to the rutile (110) peak centered at 3.24 Å. In addition, the rutile (111) peak centered at 2.19 Å also increases, indicating that after annealing to 973 K some phase transformation to rutile has occurred. Concurrently, the brookite shoulder located at 2.90 Å decreases. Unlike XRD, a variety of factors influence the pixel intensity used to generate the radial profile plots. As a result, attempts at using both the Scherrer formula and relative phase composition using the integrated peak areas failed to produce reasonable results from the SAED data in Figure 5. Further refinement of this technique to utilize these approximations is in progress.

Glancing incidence XRD measurements, as shown in Figure 6, indicate that there is no change in phase composition after annealing to 773 K. Figure 6 also includes the theoretical 2θ peaks for the rutile, brookite, and anatase peaks. The discrepancy between the SAED and XRD regarding the possible presence of brookite is likely due to an attempt to extract too much information from the SAED profiles, despite the XRD results of Zhang and Banfield,[18] which showed an increased presence of brookite after annealing at the same temperature. Due to the lack of isolated peaks for each phase in SAED, this is a possible explanation. For instance, the brookite (211) peak is seen as a small bump at 2.90 Å in the shoulder for the anatase (101) peak centered at 3.52 Å in Figure 5. In XRD, this same *hkl* peak (30.8°) is far from the anatase (101) peak centered at 25.3°, and would be clearly resolved if any significant amount of brookite was present in the sample since the theoretical intensity of this peak is 90% of the major, (210), peak at 25.3°.

Figure 7 shows the electron yield NEXAFS measurements for the oxygen K-edge after various annealing temperatures.

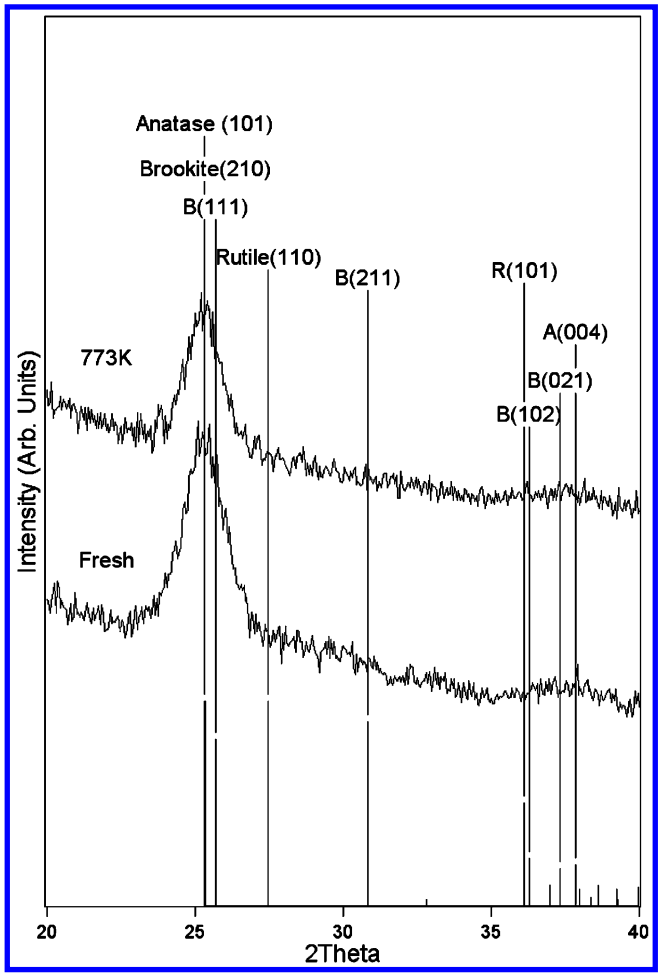

Figure 6. XRD of TiO_2 nanoparticles before and after annealing to 773 K for 4 h. Calculated rutile, brookite, and anatase peaks are included.

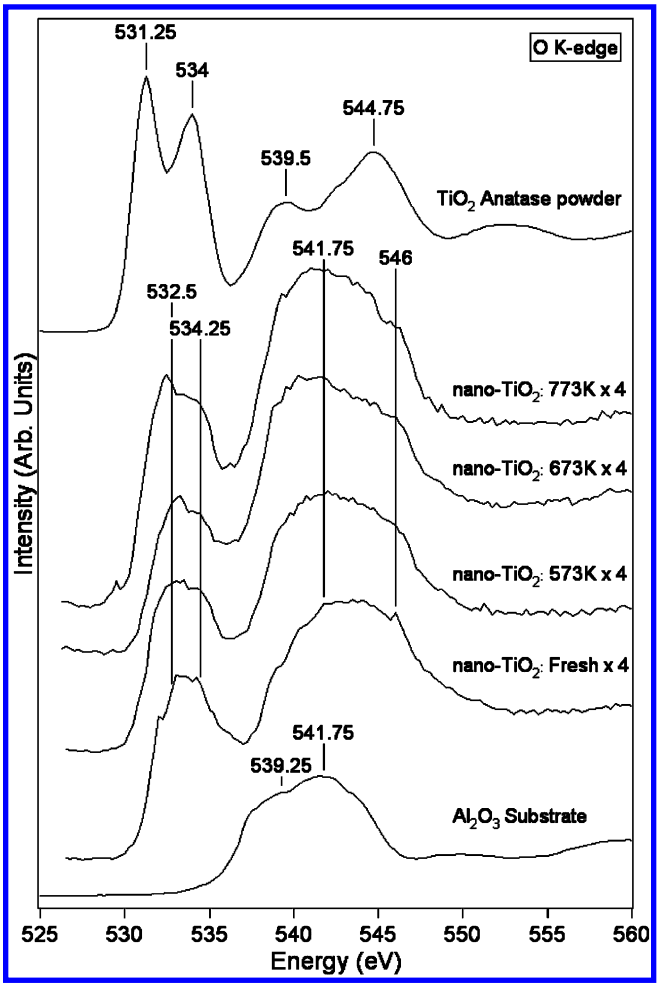

Figure 7. Electron yield O K-edge NEXAFS of powder anatase and annealed nanoparticles on an Al_2O_3 substrate.

For comparison, Figure 7 also includes the spectra of a pure anatase powder[19] and a single-crystal Al_2O_3 substrate. It is clear that the electronic structure of the nanoparticles is quite different from the bulk TiO_2 spectrum. The O K-edge features, corresponding to the transition of the O 1s electron to the $2t_{2g}$ and $3e_g$ orbitals, are located at 531.3 and 534 eV, respectively, for the bulk anatase powder.[19,20] The same features are not resolved for any of the nanoparticle samples. As discussed in the paper by Lusvardi et al.,[19] the comparison of the O K-edge features of a single-crystal TiO_2 (001) shows a reduction in the $t_{2g}-e_g$ peak splitting, as well as a shift to higher energies as the TiO_2 (001) surface is sputtered by Ar^+ ions. The lack of distinguishable e_g and t_{2g} peaks for the nanoparticle spectra, as well as the shift to higher energies, suggests that the surface of the nanoparticles may possibly be distorted due to surface defects. The features between ~537 and ~550 eV are sensitive to the long-range interaction characteristic of the O_h symmetry and are due to a covalent mixing of the O 2p and Ti 4sp states.[19] The O K-edge feature of the nanoparticles in this energy range is again different from those of bulk TiO_2, further indicating the distorted nature of the nanoparticle surfaces.

The lack of distinguishable features in the nanoparticle spectra indicates that either a long-range order does not exist for nanoparticles or the crystal structure at the surface region is distorted enough to no longer be of O_h symmetry. However, the lack of long-range order is in contrast to the SAED and XRD results, which indicate crystalline samples. Such differences are most likely due to the surface-sensitive and bulk-sensitive natures of the different techniques.

However, important for this work, the O K-edge features do not change after annealing to 773 K, suggesting a similar binding environment for TiO_2 nanoparticles after annealing to 773 K.

IV. Discussion

The as-produced phase-pure anatase particles appear spherical in nature, in contrast to the expected shape of the anatase crystal based on previous reports.[23,24] It is presumed that the sudden quenching of particles by the rotating sampler may in fact kinetically trap the anatase particles in a less favorable thermodynamic configuration. The absence of noticeable changes in the NEXAFS O K-edge features after annealing up to 773 K combined with the spherical nature of the particles after annealing to 773 K imply that the particles have not changed after annealing. The lack of any change in phase concentration after similar annealing experiments based on XRD and SAED measurements supports this conclusion.

Nanoparticle phase stability is strongly influenced by the surface free energy (S.F.E.).[21−25] As reported in the literature, the lower surface energies of both the brookite and anatase surfaces create a stability crossover where these phases are more stable than rutile despite the lower bulk free energy of the rutile phase.[22,25] As a note on nomenclature, the stability crossover point is technically an area and not a diameter, and yet all reports including this one use a spherical assumption in reporting a particle diameter threshold. Below a certain particle size,

between 15 nm listed in refs 23 and 24 and 35 nm in refs 22 and 25 depending on the method used to calculate the surface free energy, the anatase phase becomes the thermodynamically stable phase due to the effect of the surface energy.[22−25]

Particle growth will occur at elevated temperatures as particles sinter together,[21−25] but the mechanism is kinetically trapped at room temperature. Since the rutile phase for larger particles is still the global minimum on the free energy surface, anatase particles are metastable unless they are completely isolated and thus incapable of growth. This is the case inside the flame: if precursor concentration is sufficiently low that the particle mean free path dictates no particle−particle interaction, then the particles will grow in the phase that is thermodynamically stable for that particle size. This is why despite a flame temperature of ∼2200 K, pure-phase anatase particles are produced.[12] If the particles are not isolated, but in contact with additional particles, then sintering and particle growth can occur to further reduce the free energy of the system, provided sufficient energy is available to overcome any associated energy barrier. Once the particle size crosses the stability threshold, a phase change can occur further reducing the free energy.

From a catalysis perspective, it is critical to maintain both the size and phase of nanoparticles to obtain reproducible results. Therefore it is important to determine under what conditions the particles are stable, or technically, kinetically trapped. This has been investigated to some extent previously,[18] and the current study expands upon this work by using combustion synthesized phase-pure anatase particles and with the introduction of NEXAFS to compare the local binding environment with that of bulk TiO_2. The results of the current study suggest that nanoparticle anatase TiO_2 does not undergo any phase transformation or particle growth at temperatures up to 773 K for 2 h based on TEM (Figures 2 and 3), SAED (Figure 5), XRD (Figure 6), and NEXAFS (Figure 7).

This is consistent with the results of Zhang and Banfield.[18] Their results for particles of similar dimensions indicate that no particle growth occurred below 850 K, and that phase transformation to brookite was slow, indicating that sufficient energy was available to overcome any energy barrier for growth and transformation but not enough for the reaction to proceed rapidly. However, their starting material contained a significantly higher mass fraction of brookite than the starting material in this study, making a direct comparison difficult. It could be possible that the brookite, already present in ref 18, grows at a significantly faster rate than the anatase nanoparticles, and this assumption is justified due to the higher bulk free energy and surface energies of brookite compared to anatase.[25] As discussed above, it can be inferred from the available studies in the literature and the results of this study that anatase particles ∼4 nm in size are thermodynamically metastable and remain unchanged as long as surface growth mechanisms are suppressed.[21−25] After annealing to 973 K, significant increases in both particle size and rutile concentration were observed from TEM (Figure 4) and SAED (Figure 5) measurements. In addition, the shape of the TiO_2 particles has taken the form of the reduced energy of rutile, i.e., more a flat rectangle than spherical.[26]

V. Conclusions

The current paper reports the first investigation of the thermal stability of flame-synthesized TiO_2 nanoparticles. On the basis of the results and discussion described above, conclusions regarding the new insights into the thermal stability of the anatase TiO_2 nanoparticle are summarized as follows. Phase-pure anatase TiO_2 nanoparticles were synthesized by using a combustion flame with titanium tetraisopropoxide (TTIP) precursor. Through control of precursor concentration, production of ∼4 nm primary particle size can be obtained reproducibly. Subsequent thermal annealing experiments indicate thermal stability up to 773 K. TEM, XRD, and NEXAFS measurements confirm that particles remain kinetically trapped even under annealing conditions of 773 K for 2 h in air. No corresponding change in size or phase was observed with TEM, SAED, and XRD under these conditions. However, in agreement with reported observations in the literature,[21−25] annealing to 973 K leads to an increase in primary particle size and in rutile mass fraction based on SAED and a corresponding shape change to the thermodynamically favored shape for rutile.

Acknowledgment. The authors acknowledge financial support through NSF-NIRT (Grant No. DMR-0210284). We also acknowledge Brian McCandless for the glancing incidence XRD measurements and Dr. Chaoying Ni for assistance with TEM measurements. We acknowledge ExxonMobil for beamtime on NEXAFS.

References and Notes

(1) Diebold, U. *Surf. Sci. Rep.* **2003**, *48*, 53.
(2) Umebayashi, T. *J. Phys. Chem. Solids* **2002**, *63*, 1909.
(3) Nakaso, K.; Okuyama, K.; Shmida, M.; Pratsinis, S. E. *Chem. Eng. Sci.* **2003**, *58*, 3327.
(4) Gaertner, G. G.; Lydtin, H. *Nanostruct. Mater.* **1994**, *4*, 559.
(5) Beck, D. D.; Siegel, R. W. *J. Mater. Res.* **1992**, *7*, 1861.
(6) Fox, M. A.; Dulay, M. T. *Chem. Rev.* **1993**, *93*, 341.
(7) Skandan, G.; Chen, Y.-J.; Glumac, N.; Kear, B. H. *Nanostruct. Mater.* **1999**, *11*, 149.
(8) Presented By H. Wang at the 2003 Fall Meeting of Eastern States Section of the Combustion Institute, Pennsylvania State University, University Park, PA, Oct 26−29 2003.
(9) Zhang, H.; Banfield, J. F. *Am. Mineral.* **1999**, *84*, 528.
(10) Pratsinis, S. E. *Prog. Energy Combust. Sci*. **1998**, *24*, 197.
(11) Harano, A.; Shimada, K.; Okubo, T.; Sadakata, M. J. *Nanoparticle Res.* **2002**, *4*, 215.
(12) Zhao, B.; Uchikawa, K.; McCormick, J. R.; Ni, C.; Chen, J. G.; Wang, H., submitted to the 30th International Symposium on Combustion.
(13) Woolridge, M. S. *Prog. Energy Combust. Sci.* **1998**, *24*, 63.
(14) Kammler, H. K.; Madler, L.; Pratsinis, S. E. *Chem Eng. Technol.* **2001**, *24*, 583.
(15) Zhang, H.; Banfield, J. F. *Phys. Chem. B* **2000**, *104* 3841.
(16) Zhao, B.; Yang, Z.; Wang, J.; Johnston, M. V.; Wang, H. *Aerosol Sci. Technol.* **2003**, *37*, 611.
(17) Zhao, B.; Yang, Z.; Johnston, M. V.; Wang, H.; Wexler, A. S.; Balthasar, M.; Kraft, M. *Combust. Flame* **2003**, *133*, 173.
(18) Zhang, H.; Banfield, J. F. *J. Phys. Chem. B* **2000**, *104*, 3481−3487.
(19) Lusvardi, V. S.; Barteau, M. A.; Chen, J. G.; Eng, J., Jr.; Fruhberger, B.; Teplyakov, A. *Surf. Sci.* **1998**, *397*, 237.
(20) Chen, J. G. *Surf. Sci. Rep.* **1999**, *30*, 1.
(21) Penn, R. L.; Banfield, J. F. *Geochim. Cosmochim. Acta* **1999**, *63*, 1549.
(22) Zhang, H.; Banfield, J. F. *J. Mater. Chem.* **1998**, *8*, 2073.
(23) Lazzeri, M.; Vittadini, A.; Selloni, A. *Phys. Rev. B* **2001**, *63*, 155409.
(24) Lazzeri, M.; Vittadini, A.; Selloni, A. *Phys. Rev. B* **2001**, *65*, 19901-(E).
(25) Ranade, M. R.; Navrotsky, A.; Zhang, H. Z.; Banfield, J. F.; Elder, S. H.; Zaban, A.; Borse, H.; Kulkarni, S. K.; Doran, G. S.; Whitfield, H. J. *Proc. Natl. Acad. Sci. U.S.A.* **2002**, *April 30*, 6476.
(26) Ramamoorthy, M.; Vanderbilt, D.; King-Smith, R. D. *Phys. Rev. B* **1994**, *49*, 16721.